

Monitoring of Freezing Water or Melting Ice in Aircraft Fuel Tanks and Fuselages by Acoustic Emission

HELGE PFEIFFER, DAVID SEVENO, JOHAN REYNAERT,
PIETER JAN JORDAENS, ÖZLEM CEYHAN
and MARTINE WEVERS

SUMMARY

It is a mostly overlooked phenomenon in physical chemistry that matter produces characteristic sound emissions when passing through a phase transition. The origin of this sound is not yet fully understood, but it is certain that sudden changes in volume, cracks, friction between crystallites and other sources must be considered, but a generally accepted theory of the "sound of phase transitions" is lacking. But even if the cause is not completely clear, this phenomenon can be used to detect the presence of these substances in technical structures. This is important, for example, in the case of water and ice in aircraft fuel tanks. Water arising from contamination and condensation is frequently found in fuel tanks and regular drainage procedure are important to guarantee the safety of systems and structures. While ice dispersed in the kerosene phase can seriously hinder the combustion process, blocks of ice can cause serious crack formation as in valves and tubes.

A practical problem with all drainage procedures after flights at freezing conditions is the right time to start that process. Starting too early would mean that the remaining ice cannot be removed and waiting too long is an economic problem because it increases the aircraft's downtime. Unfortunately, there is no technology yet that tells mechanics when all the water has melted. It would be beneficial for maintenance teams to find the right time to drain, and acoustic emissions from the melting ice would be the ideal tool to determine this moment. For this purpose, acoustic sensors are attached to the skin of the tank walls, and the acoustic signals from the ice are intense enough to propagate through media, the aluminum sheets and coating. In this way, the completion of the ice melt is determined by the time at which the acoustic emission stops.

We present measurements on a laboratory scale, results from a realistic climate chamber on a tank model and the first results from a campaign on an operational aircraft (Airbus A330). We were able to show that relevant amounts of melted ice can be reliably determined, e.g., 30 ml of water under the kerosene phase in a replica fuel tank generate about 200,000 distinguishable signals, in our case these signals are acoustic transients. This is quite sufficient to obtain the desired information about the state of the

melting ice. In addition, to address other structures, results of ice melting and water freezing processes on an aircraft fuselage model are presented.

1 INTRODUCTION

1.1 Phase Transitions and Acoustic Emission

Phase transitions can be associated with acoustic events [1, 2]; and there is for example the characteristic cracking sound that occurs during ice melting, for instance in the case of an ice cube in a drink. It is however important to note that for practical applications, the focus is mainly on the ultrasonic frequency band. Those acoustic events, usually called “Acoustic Emission (AE)” are in general terms generated by transient stress relaxations processes within matter. Although little research has been dedicated to the “sound of phase transition” in the past, there are some explanations that have been proposed [1]. A first explanation refers to steric mismatches due to inhomogeneous thermal expansions that creates stresses between areas at different temperature levels. These thermal stresses cause cracks along the crystal interfaces with different lengths and energy scales. A second source of acoustic emission refers to the spontaneous volume changes of ice microcrystals transitioning into a liquid state and vice versa.

The research in that area is not only limited to water; also other compounds such as p-cresol, or Methoxybenzylidene-4-n-butylaniline liquid crystal have been investigated [2]. One observation was that the acoustic activity seems to be more intense when the transition to a higher density state occurs. Consequently, in the case of water, more events are observed during melting than during freezing. Related phenomena are also observed at crystallisation and solvation processes, which are also accompanied by AE [publication under preparation].

1.2 Water Drainage and Remaining Ice in Fuel Tanks

Recently, we used the AE of ice to detect residual ice in aircraft tanks [3]. The AE generated during the melting process in the fuel tank can be detected by externally mounted sensors so that the optimum time for draining the water from the tank can be determined.

Water in aircraft fuel tanks can be the result of a variety of factors, such as leaks, condensation, or fueling with contaminated fuel. Water, especially ice, causes a variety of issues that can potentially affect aircraft safety and performance [1]. Engine failures are one of the main issues, as water can have a significant negative impact on the combustion process. In addition, water in fuel systems may lead to corrosion and important components such as fuel pumps, fuel lines and valves may be damaged. It is also known that water promotes the growth of microbial organisms such as bacteria and fungi, which in turn can clog fuel filters and damage fuel system components, as well leading to microbial corrosion. Finally, when water freezes at low temperatures, especially at high altitudes, it can form ice crystals, which in turn can clog fuel lines or injectors, leading to engine failure or reduced engine performance. Ice can thus actually occur in various forms, e.g., as "snow-like" ice or as blocks of ice on the tank walls. To



Figure 1. Setup for monitoring ice melting by acoustic emission sensors located close to the water drain valves at the wing sections (Airbus A330).

reduce these risks, airlines must take measures such as properly draining the fuel tank to remove the water before flight (Figure 1).

The timing to start water drainage is a major challenge. All the ice has to be melted, but due to the large mass and volumes within the tank of an aircraft, this can be a long process. A rule of thumb for the Airbus A330 is that one has to wait between 10 and 13 hours before start draining, depending on summer or winter. However, one can assume that this waiting time is actually much too long and just a result of safety considerations. If the mechanics would however be able to determine completion of melting, they could start draining much earlier.

1.3 Acoustic Emission for Monitoring Structures and Water Melting

To find the optimal time for water drainage, acoustic emission (AE) technology offers a very interesting option. AE is already well-established in the field of non-destructive testing (NDT) and monitoring, especially condition and process monitoring, for defect detection, but also in basic research [3-5]. Such as mentioned above, the use of the AE technology for timing water drainage is based on the fact that ice emits sounds over a wide frequency range during the phase transition to water (the melting), and even during freezing of water AE is produced: the liquefaction or solidification [2].

Given properly chosen thresholds, the AE coincides with the start and completion of the melting or freezing process, making it an ideal method for determining the optimal time to start drainage. Note that the sensors can be placed on the outer surface of the tank walls, as the sound waves propagate relatively smoothly through the aluminum tank material. Furthermore, since the water collects at the deepest point of the tank and this position is known, no complicated localization procedures are required.

2 MATERIALS AND METHODS

The main component of the experimental set-up is a Vallen AMSY-6 system designed for the detection and analysis of Acoustic Emission (AE) signals. A specific advantage of the system is its portability, i.e., it can be flexibly deployed at different

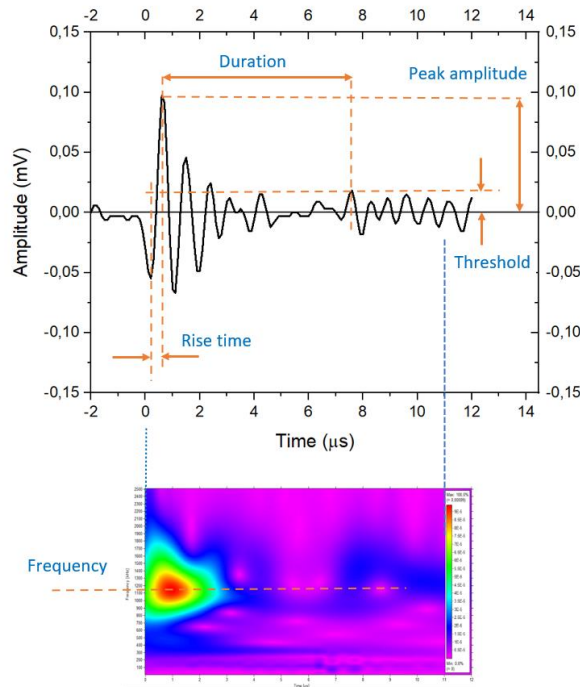


Figure 2. Representative waveform recorded with AE equipment, including a wavelet representing the time evolution of frequency content (obtained by the Vallen ASMY-6 system). The frequency scale for the wavelength is in the range of 100 – 2500 kHz, and the main frequency is in the range of 1,3 MHz.

locations without compromising performance. The software-controlled analogue frequency filtering was set for the frequency range from 50 kHz to 1600 kHz. The acquisition rate is set to 2.5 MS/s. To optimize signal quality and minimize noise, an AEP4 preamplifier (34 dB) is used, placed between the sensor and the AMSY-6 recording unit. Coaxial cables with an impedance of 50 Ohm were applied to connect the various components. The VS30-V acoustic emission sensor had a flat frequency range of 25 to 85 kHz. It was connected to the structure via a mechanical clamp, respectively suction cups. To allow sufficient acoustic contact, vacuum grease was used between the surface of the sensor and the material under investigation.

Figure 2 provides a typical waveform processed with the AE Vallen software, using parameters, such as amplitudes and duration times. In the present analysis, only two parameters are considered: a) the number of hits (threshold crossing) as a function of time and b) the number of hits in an respective amplitude range. The latter analysis leads to a distribution function that is frequently linear in a double logarithmic representation and the slope is described by a so-called b -value defined by $N/N_t = (A/A_0)^{-b}$, where N is the number of hits above the amplitude A , N_t is the total number of hits observed at the reference amplitude A_0 . The b -value is assumed to reflect the physical properties of the material under investigation, such as its microstructure, damage accumulation, and stress state, and in our case, the properties of the phase transition under its specific boundary conditions (see also Chen [8]). For practical applications, aside of the detailed physical meaning, we hope to use that parameter to distinguish between environmental noise and signals from ice melting.



Figure 3. Left) Generic replica of a section of a fuel tank. The dashed red lines indicate the characteristic inclination of the wings (modelled on an A330), and the model aircraft schematically shows the analogous orientation of the underside of the tank section, so that its approximate position in relation to the wing profile can be assessed (the aircraft was taken from the MS Word 3D model), Right, replica of a fuselage panel.[9].

A replica of a tank section was manufactured at the premises of Brussels Airlines (Figure 3, left) with dimensions of 100 cm × 50 cm × 20 cm. It was made using sheets of a typical aircraft aluminum alloy (Al2024-T3) with a thickness of 2 mm welded on a base plate of 8 mm. The replica was coated with an epoxy primer on the inside and bottom and a polyurethane coating on the outside and bottom to imitate the acoustic properties of real aircraft tanks. The replica was mounted at angles typical of the wing position, with a dihedral angle of approximately 6° and an angle of attack of 2-3°. So, water accumulates in typical position at a predefined lowest point. We added 30 ml of water and covered it with approximately one liter of kerosene. Next, we fixed an AE sensor outside the tank at its lowest point. The entire replica was then moved into the climate test chamber and the temperature was adjusted to -16 °C.

For the replica of the fuselage panel (figure 3, right), aluminum alloy sheets of Al2024-T3 with a thickness of 1 mm were used and coated according to standard procedures. It contained stringer and stiffener elements that were riveted. It has approximate dimensions of 1 m x 0,8 m. For tests at realistic temperature conditions, the Sirris Large Climate Test Lab in Antwerp (Belgium) was used. This lab is designed for testing large and heavy equipment under extreme weather conditions such as temperature ranges from -60°C to +60°C, including thermal cycling, humidity levels up to 95% RH, and icing.

3 RESULTS AND DISCUSSION

3.1 Freezing and melting in replica tank section

When the replica tank section model was moved into the climate test chamber, data recording was started at a threshold level of 37.1 dB to ensure no relevant noise signals were captured. Figure 4, left shows the graphical representation of acoustic data of the freezing process of 30 ml of water under a kerosene layer given by the number of hits as a function of time. Start and completion of freezing was in parallel also confirmed by visual observations. After approximately 2000 seconds which were needed to cool

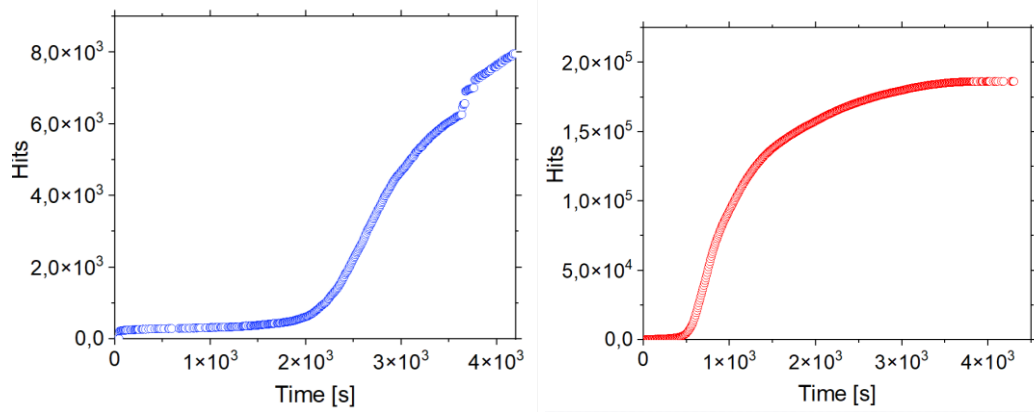


Figure 4. Number of hits recorded during freezing (left), as well as melting (right) of 30 ml water below a layer of kerosene. Note the different y-axis scales.

down the system, we observed the start of the freezing process characterized by a burst of incoming AE signals (figure 4, left). After approx. 2000 seconds, no further significant AE signals were detected because the entire water phase had frozen, as confirmed by visual observations. Then, the replica was removed from the climate test chamber into an outside area with an approximate temperature of 12°C . After 10 minutes, melting started as observed visually but also detectable by intense acoustic activity; finally, 200,000 hits were recorded (figure 4, right). After almost one hour, the melting was completed.

3.2 Freezing and Melting on a Fuselage Panel

Tests in the previous subchapter focused on residual ice under the kerosene phase in a fuel tank but exploring the acoustic behavior of water droplets on the fuselage is also highly relevant. One could imagine aircraft waiting on the ground during rainy conditions and sub-zero temperatures, where acoustic events from rainwater and freezing water would mix. In this example, the fuselage plate is first cooled within the climate test chamber to approximately -18°C , and an AE sensor is clamped at one corner of the plate to collect the AE data from the entire surface. When the plate was situated long enough in the climate test chamber, around 30 minutes, we initiated the AE data recording and set a threshold to ensure no noise signals from external sources were captured. A specialized sprayer was then used to deposit water droplets over the entire surface of approximately one square meter, with the water temperature at about 10°C . At the data recorded during spraying and freezing (figure 5, left) a typical pattern is observed during the spraying process onto this supercooled fuselage plate.

There is a steep increase in the number of accumulated hits over a period of approximately 50 seconds, coinciding with the onset of freezing. Finally, from the number of accumulated hits one can estimate that from the ~ 4700 hits recorded ~ 3400 can be assigned to the ice freezing process. It is important to note that, in this experiment, thousands of droplets were distributed over the fuselage replica, and these droplets do not freeze collectively, but rather at separate moments. Therefore, separate steps in the sigmoidal behavior are frequently observed, indicating the freezing of more individual water clusters. This is usually in contrast with melting processes

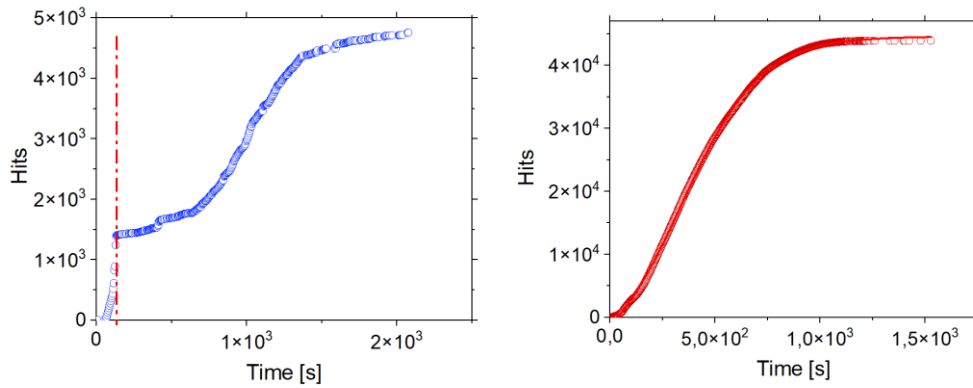


Figure 5. Number of hits recorded during the spraying and freezing (left) and melting (right) of ice droplets on a fuselage panel. The dashed line at the left side gives the moment when spraying was finished, the red line in the right plot represents a best-fit line calculated according to the Boltzmann equation ($R=0,9995$). Note the different y-axis scales.

where curves appear smoother. After the freezing process was completed, (after approximately 2200 seconds), which was indicated by the flattening of sigmoidal curve and confirmed by visual observations, the data recording could be stopped. The fuselage plate was then removed from the climate test chamber and placed at an outside area with a temperature of approximately 15 °C.

The accumulated hits for melting (figure 5, right) show an almost perfect sigmoidal behaviour. The accomplishment of the ice melting could easily be identified from the flattening of the sigmoidal curve and was reached after 45,000 hits. The curve can be fitted according to a standard Boltzmann equation, $y=A_2+(A_1-A_2)/(1+exp(x-x_0/dx))$, where y are the number of hits, A_1 and A_2 relate to the amount of hits before and after the transition, x_0 describes the mid of the transition process (342 s) and dx is an expression for the width of the curve (189 s), thus for the duration of the transition as such. Note, the number of hits obtained during melting is more than ten times higher than during the freezing process. This behavior has been observed frequently in previous experiments. The explanation is that phase transitions that lead to a phase with a higher density create more acoustic activity [2].

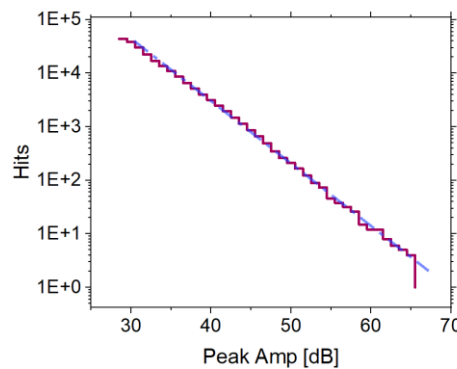


Figure 6. The distribution function for the melting process of ice droplets on a fuselage panel.

Additionally, the distribution function, here the number of hits versus amplitude, shows an almost perfect single line with a slope of $b=2.3$. In contrast to the tank melting droplets were individually distributed at the plate.

4 SUMMARY AND CONCLUSIONS

The application of AE technology to determine the completion of ice melt in engineering structures was demonstrated. It can be stated that ice freezing and melting is governed by a distribution function with $b=2,3 \pm 0,5$. Values in that range were previously provided for diverse crack-related phenomena in rocks [10]. To test the effectiveness of the AE technology on operational aircraft, a campaign on Airbus A330 is currently ongoing. Any remaining obstacles to implement this technology into an operational environment appear to be minor and a question of appropriate engineering targeting simple handling of sensors, data transmission and recording including an easy-to-use software.

5 ACKNOWLEDGMENTS

Research leading to these results has received funding from the “NDTonAIR” project (Training Network in Non-Destructive Testing and Structural Health Monitoring of Aircraft structures) under the action: H2020-MSCA-ITN-2016- GRANT 722134 as well as the “Fighting Icing” project (COOCK – VLAIO, Belgium).

6 REFERENCES

- [1] D.M. Kuznetsov, A.N. Smirnov, A.V. Syroeshkin, New Ideas and Hypotheses: Acoustic emission on phase transformations in aqueous medium, *Russian Journal of General Chemistry* 78 (2008) 2273-2281.
- [2] T. Sawada, Y. Gohshi, C. Abe, K. Furuya, Acoustic emission from phase transition of some chemicals, *Anal. Chem.* 57 (1985) 1743-1745.
- [3] M.S. Alam, F. Gulshan, Q. Ahsan, M. Wevers, H. Pfeiffer, A.-W. van Vuure, L. Osorio, I. Verpoest, Development of Methodology to Assess the Failure Behaviour of Bamboo Single Fibre by Acoustic Emission Technique, *Journal of The Institution of Engineers (India): Series D* 98 (2017) 9-17.
- [4] S.V. Lomov, M. Karahan, A.E. Bogdanovich, I. Verpoest, Monitoring of acoustic emission damage during tensile loading of 3D woven carbon/epoxy composites, *Text. Res. J.* 84 (2014) 1373-1384.
- [5] M. Wevers, S. Van Huffel, S. Vandenplas, J.M. Papy, Acoustic emission monitoring using a polarimetric Single Mode optical fibre sensor, *Int. J. Materials and Structural Integrity* 1 (2007) 148-160.
- [6] M. Stamm, H. Pfeiffer, J. Reynaert, M. Wevers, Using Acoustic Emission Measurements for Ice-Melting Detection, *Applied Sciences* 9 (2019).
- [7] M. Sohail, H. Pfeiffer, M. Wevers, Addressing Safety concerns in Hybrid Electric Aircrafts: In-Flight Icing Detection, Moisture Detection in Fuselage and Electrical Wiring and Interconnect System (EWIS), 11th EASN International Conference Virtual, 2021.
- [8] D. Chen, C. Xia, H. Liu, X. Liu, K. Du, Research on b Value Estimation Based on Apparent Amplitude-Frequency Distribution in Rock Acoustic Emission Tests, *Mathematics*, 2022.
- [9] H. Pfeiffer, J. Reynaert, D. Seveno, P.J. Jordaens, Ö. Ceyhan, M. Wevers, Monitoring melting ice formations in aircraft fuel tank by acoustic emission, *SAE International Conference on Icing of Aircraft, Engines, and Structures* Vienna, Austria, 2023.
- [10] M.V.M.S. Rao, K.J. Lakshmi, Analysis of b-value and improved b-value of acoustic emissions accompanying rock fracture, *Curr. Sci.* 89 (2005).